Hindawi
Shock and Vibration
Volume 2019, Article ID 8103216, 13 pages
https://doi.org/10.1155/2019/8103216

Research Article

Undersampled Blade Tip-Timing Vibration Reconstruction under Rotating Speed Fluctuation: Uniform and Nonuniform Sensor Configurations

Zhongsheng Chen,[1,2] **Jing He**,[1] **and Chi Zhan**[2]

[1]*College of Electrical & Information Engineering, Hunan University of Technology, Zhuzhou 412007, Hunan, China*
[2]*Science and Technology on Integrated Logistics Support Laboratory, National University of Defense Technology, Changsha 410073, Hunan, China*

Correspondence should be addressed to Zhongsheng Chen; chenzs_hut@sina.com and Jing He; hejing@263.net

Received 3 February 2019; Revised 10 May 2019; Accepted 17 July 2019; Published 14 August 2019

Academic Editor: Athanasios Chasalevris

Blade tip-timing (BTT) is a promising method of online monitoring rotating blade vibrations. Since BTT-based vibration signals are typically undersampled, how to reconstruct characteristic vibrations from BTT signals is a big challenge. Existing reconstruction methods are mainly based on the assumption of constant rotation speeds. However, rotating speed fluctuation is inevitable in many engineering applications. In this case, the BTT sampling process should be nonuniform, which will cause existing reconstruction methods to be unavailable. In order to solve this problem, this paper proposes a new reconstruction method based on nonlinear time transformation (NTT). Firstly, the effects of rotating speed fluctuation on BTT vibration reconstruction are analyzed. Next, the NTT of BTT sampling times under rotating speed fluctuation is presented. Then, two NTT-based reconstruction algorithms are derived for uniform and nonuniform BTT sensor configurations, respectively. Also several evaluation metrics of BTT vibration reconstruction under rotating speed fluctuation are defined. Finally, numerical simulations are done to verify the proposed algorithms. The results testify that the proposed NTT-based reconstruction method can reduce effectively the influence of rotating speed fluctuation and decrease the reconstruction error. In addition, rotating speed fluctuation has more bad effects on the reconstruction method under nonuniform sensor configuration than under uniform sensor configuration. For nonuniform BTT signal reconstruction under rotating speed fluctuation, more attentions should be paid on selecting proper angles between BTT sensors. In summary, the proposed method will benefit for detecting early blade damages by reducing frequency aliasing.

1. Introduction

High-speed rotating blades are key mechanical moving components in turbomachinery, such as engine compressor and turbine blades. In particular, these blades are often exposed to extremely severe conditions of vibrations, centrifugal forces, and temperatures. High cycle fatigues due to low stress and high-frequency vibrations always result in different blade damages or faults. Moreover, severe vibratory stresses may induce blade cracks. In practice, cracks in rotor blades will often cause catastrophic failures [1]. Statistics data have shown that over 60% of the overall faults are caused by vibrations. Furthermore, blade faults have accounted for more than 70% of the overall vibration-induced faults [2]. Thus, online vibration monitoring for detecting incipient cracks in high-speed rotor blades during operation is an important requirement from the perspective of safety, reliability, availability, and maintenance [3, 4].

Blades rotate continuously during working, so it is a big challenge to carry out online vibration monitoring. In recent years, more and more interest in blade vibration monitoring is arising. Existing methods can be divided into two classes. The first one is called as contact measurement. A common

contact measurement method is to mount a strain gauge on a blade surface and obtain vibration signals by using a slip-ring [5, 6]. But this way has several shortcomings. Firstly, a strain gauge needs to be attached to each blade face. That is to say, each strain gauge can only be used to monitor a blade. In particular, a strain gauge should in return affect vibration characteristics of the blade. Secondly, the life of a strain gauge is often limited due to serious operation environment and not enough for enduring long time. As a result, it needs to replace strain gauges periodically and the cost is great. Thirdly, a high-speed slip ring is needed for transmitting signals and its expense is also very high. In order to overcome the shortcomings of contact measurement methods, more and more researchers are studying noncontact blade vibration monitoring methods. Nowadays, blade tip-timing (BTT) has become a promising approach of noncontact vibration monitoring [7–9]. A BTT method always uses the times at which the blade tips pass the casing-mounted probes to obtain all-blade vibrations simultaneously. When there are no blade vibrations, passing times of each blade will only be a function of rotating speed, blade tip radius, and circumferential probe positions. Otherwise, the blades will pass the probes earlier or later, so that blade passing times deviate from those obtained in the undisturbed condition, leading to a time difference series. Based on this series, we can calculate all-blade vibration displacements. But its main drawback is that the sampling frequency completely depends on the rotating speed and the number of installed sensors. In practice, the number of BTT sensors is small due to the restrictions of spaces and costs, so the sampling frequency of blade vibration signals is always much less than natural frequencies of blades. In this case, blade vibration signals are well undersampled and need to be reconstructed. How to reconstruct vibration characteristics from undersampled BTT signals is a big challenge. Few works have been done. Bendali et al. proposed a BTT signal reconstruction method based on the Shannon theorem [10]. However, practical BTT signals are not truly band-limited, so aliasing still exists in reconstructed signals. In order to overcome this issue, Chen et al. proposed an improved BTT signal reconstruction based on the Shannon theorem and wavelet packet transform [11].

According to classical theory of BTT measurements, the rotating speed is expected to be invariant. Otherwise, the time difference series is inaccurate, which will cause spectral errors. In many engineering applications, however, the rotation speed is impossible to be a constant due to unstable airflow, load instability, and other influencing factors. Though either arrival times of all blades at one or multiple revolutions or few blades around the blade under consideration are used to define expected arrival time, we cannot make sure that the effect of rotating speed fluctuation can be reduced completely. Under large rotating speed fluctuations, spectral errors will appear in reconstructed blade vibrations using existing algorithms. In this case, it is much difficult to detect incipient blade damages because early damages also just cause small spectral shifts. In particular, vibration reconstruction may fail completely when the rotating speed fluctuates too much. Thus, it is much significant to study blade vibration reconstruction under rotating speed fluctuations. To our best knowledge, little similar work has been done to solve this problem. Bouchain et al. presented a new sparse signal model for tip-timing spectral analysis that considered rotating variations, which was then solved by alternating direction method of multipliers with a ℓ^1 regularization [12]. In this case, frequency aliasing was reduced. But this method is a little complex.

The goal of this paper is to advance the previous works [11, 13, 14] and explore a new BTT vibration reconstruction method under rotating speed fluctuation. Firstly, the effect of rotating speed fluctuation on BTT measurements is equivalent to a random nonuniform sampling process. Then, nonlinear time transformation is introduced to transform the random nonuniform sampling process into a uniform sampling process. Based on this, new BTT vibration reconstruction algorithms are proposed for uniform and nonuniform BTT sensor configurations, respectively. The remaining paper is organized as follows. In Section 2, effects of speed fluctuation on BTT vibration reconstruction are discussed and evaluation metrics of BTT vibration reconstruction methods are defined. Next, nonlinear time transformation of BTT sampling times under rotating speed fluctuation is presented in Section 3, which is the basis of this paper. In Section 4, two classes of NTT-based BTT vibration signal reconstruction algorithms under rotating speed fluctuation are proposed for uniform and nonuniform BTT sensor configurations, respectively. Then numerical simulations are carried out to verify the proposed methods in Section 5. Finally, conclusions are summarized in Section 6.

2. Effects of Rotating Speed Fluctuation on BTT Vibration Reconstruction

2.1. Basic Principles of BTT-Based Blade Vibration Monitoring. Basic principle of a BTT measurement system is shown in Figure 1. Firstly, I BTT sensors are embedded into a stationary casing around a bladed-disk with K blades. In practice, BTT sensors can be optical fiber, eddy current, and microwave or capacitive sensors. At the same time, an once-per-revolution sensor is mounted in front of the shaft as a reference sensor. The angular positions of the i^{th} $(1 \le i \le I)$ BTT sensor and the k^{th} $(1 \le k \le K)$ blade are denoted as α_i and θ_k, respectively.

The basis of BTT methods is to measure the arrival times when each blade passes each BTT sensor. When there are no blade vibrations under ideal conditions, the passage times of each blade will only be a function of rotating speed, blade tip radius, and its circumferential position. Obviously, these parameters are fixed, so the blade passage times are also deterministic. However, when blade vibrations happen, the blades will pass BTT sensors earlier or later than normal values. Thus, the blade passing times will deviate from those under undisturbed conditions and a time difference series will be generated for each blade. Then, vibration displacements of each blade can be calculated based on these time differences. Obviously, the BTT method can be used to measure all-blade vibration displacements, which is much

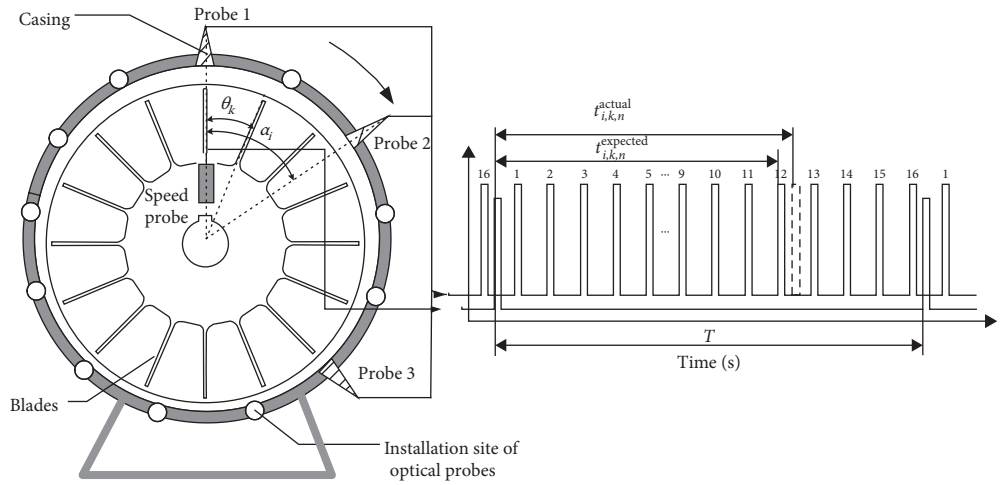

Figure 1: Basic principle of the BTT method.

superior to contact measurement methods. The details are summarized as follows.

Let the bladed-disk rotate clockwise at a constant speed. Under ideal conditions, the expected arrival times of the k^{th} blade passing the i^{th} BTT sensor can be calculated as

$$t^{\text{expected}}_{i,k,n} = \frac{1}{2\pi f_{\text{r}}}\left[2\pi(n-1) + \alpha_i - \theta_k\right], \quad n = 1, 2, \ldots, N, \tag{1}$$

where f_{r} is the rotating frequency and n denotes the n^{th} revolution.

The actual arrival times of the k^{th} blade passing the i^{th} BTT sensor are measured as $t^{\text{actual}}_{i,k,n}$. Then, the time difference series is calculated as

$$\Delta t_{i,k,n} = t^{\text{expected}}_{i,k,n} - t^{\text{actual}}_{i,k,n}. \tag{2}$$

Furthermore, vibration displacements of the k^{th} blade measured by the i^{th} BTT sensor can be represented as

$$d_{i,k}[n] = 2\pi f_{\text{r}} R \Delta t_{i,k,n} = 2\pi f_{\text{r}} R\left(t^{\text{expected}}_{i,k,n} - t^{\text{actual}}_{i,k,n}\right), \tag{3}$$

where R is the blade tip radius.

It can be seen that $I \times N$ vibration displacements of each blade are measured during N revolutions. Obviously, the sampling frequency f_{BTT} is equal to $I \times f_{\text{r}}$ if the BTT sensors are mounted uniformly. In engineering applications, the number of BTT sensors I is often small due to the restrictions of spaces and costs, so the sampling frequency f_{BTT} is always less than the natural frequency of a blade. Thus, BTT-based blade vibration signals are typically undersampled. In this case, it is difficult to obtain true vibration characteristics of a blade and detect early blade damages.

2.2. Problem Statements of BTT Vibration Reconstruction under Rotating Speed Fluctuation. As mentioned before, BTT blade vibration signals are undersampled, so they need to be reconstructed. Unfortunately, the rotating frequency f_{r} should be a constant in equations (1) and (3), otherwise measured vibration displacements are not accurate. In practice, however, this assumption is hardly to be satisfied due to many factors, such as variable loads, unstable airflows, and rotor unbalances. Thus, rotating speed fluctuation always exists, which will bring severe obstacles to BTT methods. The details are shown as follows.

When considering rotating speed fluctuation, the rotating frequency f_{r} should be a random variable, instead of a constant. That is to say, it can be represented as a function of time t, e.g., $f_{\text{r}}(t)$,

$$f_{\text{r}}(t) = \overline{f}_{\text{r}} + \Delta_f(t), \tag{4}$$

where $\overline{f}_{\text{r}}$ is the mean of $f_{\text{r}}(t)$ and $\Delta_f(t)$ is the random deviation of the rotating frequency.

Substituting equation (4) into equation (1), we will have

$$\widetilde{t}^{\text{expected}}_{i,k,n} = \frac{1}{2\pi\left[\overline{f}_{\text{r}} + \Delta_f(t)\right]}\left[2\pi(n-1) + \alpha_i - \theta_k\right]. \tag{5}$$

Thus, the expected arrival times $\widetilde{t}^{\text{expected}}_{i,k,n}$ depend on the rotating speed fluctuation $\Delta_f(t)$. Furthermore, the actual arrival times can be expressed as

$$\widetilde{t}^{\text{actual}}_{i,k,n} = \frac{1}{2\pi\left[\overline{f}_{\text{r}} + \Delta_f(t)\right]}\left[2\pi(n-1) + \alpha_i - \theta_k - \frac{\widetilde{d}_{i,k}[n]}{R}\right]. \tag{6}$$

It can be seen that the actual arrival times depend on the rotating speed fluctuation $\Delta_f(t)$ and blade vibration displacements $\widetilde{d}_{i,k}[n]$. Similar to equation (3), blade vibration displacements under rotating speed fluctuation can be represented as

$$\widetilde{d}_{i,k}[n] = 2\pi R\left[\overline{f}_{\text{r}} + \Delta_f(t)\right]\left(\widetilde{t}^{\text{expected}}_{i,k,n} - \widetilde{t}^{\text{actual}}_{i,k,n}\right). \tag{7}$$

In existing reconstruction algorithms [10, 11], the series $d_{i,k}[n]$ is used to recover true vibration characteristics of the k^{th} blade. Due to rotating speed fluctuation, however, $\widetilde{d}_{i,k}[n]$ has to be used instead of $d_{i,k}[n]$. In this case, it brings several challenges to existing reconstruction methods. The first one is that the expected arrival times are unknown and random, so that the time difference series is not accurate. The second

one is that blade vibration displacements are directly related to the rotating frequency, so that $d_{i,k}[n]$ is also not accurate. The third one is that the BTT sampling process is nonuniform, even though BTT sensors are mounted uniformly around the casing. Therefore, new reconstruction algorithms should be explored for BTT-based blade vibration monitoring, which has been never reported according to our best knowledge.

2.3. Evaluation Metrics of BTT Vibration Reconstruction under Rotating Speed Fluctuation. In order to evaluate the performance of BTT vibration reconstruction methods, some metrics should be defined and calculated. In this paper, two classes of metrics are proposed and defined as follows, including the unevenness of rotating speed (URS) and the normalized spectral kurtosis (NSK).

The unevenness of rotating speed (URS) is proposed to characterize the degree of rotating speed fluctuation, which is defined as

$$\mathrm{URS} = \frac{\left(f_{\mathrm{r}}^{\max} - f_{\mathrm{r}}^{\min}\right)}{\overline{f}_{\mathrm{r}}}, \tag{8}$$

where $f_{\mathrm{r}}^{\min}$, $f_{\mathrm{r}}^{\max}$, and $\overline{f}_{\mathrm{r}}$ are the minimum, maximum, and mean rotating frequencies, respectively.

The normalized spectral kurtosis (NSK) for a multifrequency vibration signal and spectral energy concentration can be used to characterize the reconstruction performance. The more prominent the characteristic frequencies are, the better is the reconstruction performance. Thus, the spectral kurtosis is proposed to measure the reconstruction performance, which is defined as

$$k_{\mathrm{ur}} = \frac{E\left[F(\omega) - \mu_{\mathrm{F}}\right]^4}{\sigma_{\mathrm{F}}^4}, \tag{9}$$

where μ_{F} and σ_{F} are the mean and standard deviation of spectrum, respectively. Furthermore, in order to eliminate the effects of uncertainties, a normalized spectral kurtosis is defined as

$$S_k = \frac{k_{\mathrm{ur}}}{\widehat{k}_{\mathrm{ur}}}, \tag{10}$$

where k_{ur} and $\widehat{k}_{\mathrm{ur}}$ are the spectral kurtosis of reconstructed vibration signals under rotating speed fluctuation and no fluctuation, respectively. The more close to 1 is S_k, the smaller is the reconstruction error. Thus, S_k is selected to evaluate the performance of BTT vibration reconstruction methods in this paper.

3. Nonlinear Time Transformation of BTT Sampling Times under Rotating Speed Fluctuation

In this paper, speed fluctuation can be equivalent to random variations of BTT sampling times around a central value. In this case, the issue can be transformed to reconstruct a random and nonuniformly sampled vibration signal, even though all BTT sensors are mounted uniformly.

With the help of revolution sensors, random variations of sampling times u_n can be calculated. Then, true vibration signal $d(t)$ is sampled at $t = nT + u_n$, instead of at uniform sampling times nT. Here, T is the average period which can be calculated as $T = 1/\overline{f}_{\mathrm{r}}$. The remaining problem is to determine $d(t)$ by using $d(nT + u_n)$. Therefore, nonlinear time transformation (NTT) is introduced to solve it [15]. Firstly, a continuous-time function $\lambda(\tau)$ is defined so that $\lambda(nT) = u_n$. Then, a nonlinear time transformation is built between the BTT sampling timeline t and the other timeline λ as follows:

$$t = \tau + \lambda(\tau). \tag{11}$$

Let $\tau = nT$, then $d(nT + u_n) = d(\tau + \lambda(\tau))|_{\tau=nT}$. Interestingly, nonuniform BTT sampling times $nT + u_n$ in the t domain are equivalent to uniform sampling times nT in the τ domain by using nonlinear time transformation, as shown in Figure 2.

Furthermore, a continuous-time function $g(\tau)$ is defined as follows:

$$g(\tau) = d(\tau + \lambda(\tau)). \tag{12}$$

Then we will have

$$g(nT) = d(nT + \lambda(nT)). \tag{13}$$

Thus, true vibration signals are sampled uniformly in the τ domain. This conclusion will greatly facilitate vibration signals reconstruction under rotating speed fluctuation.

4. NTT-Based BTT Vibration Signal Reconstruction Algorithms under Rotating Speed Fluctuation

We all know that high cycle fatigue (HCF) is a common failure mode of high-speed rotating blades. Generally speaking, blade vibrations are major reasons of generating HCFs, which can be classified into synchronous and asynchronous vibrations. Up to now, many studies have been done on monitoring asynchronous vibrations using uniformly-mounted BTT sensors [9, 10]. Later, Hu et al. proposed an undersampled BTT signal reconstruction method of monitoring synchronous vibrations using nonuniformly mounted BTT sensors [14]. In this section, the authors will advance the previous work [14] to consider both uniform and nonuniform BTT sensor configurations under rotating speed fluctuation.

4.1. Uniform BTT Sensor Configuration. It is assumed that the I BTT sensors are mounted uniformly. According to equation (16), $g(\tau)$ is sampled uniformly at the time points $\tau = nT$. Then, we can use the proposed method in [13] to reconstruct $g(\tau)$. The details are summarized as follows. For blade vibration monitoring, its natural frequencies are key parameters, which can be estimated in advance by using numerical or experimental analysis. Let f_0 be the targeted central frequency which can be close to natural frequencies, then we can only focus on a real band-pass signal $g(\tau)$ with

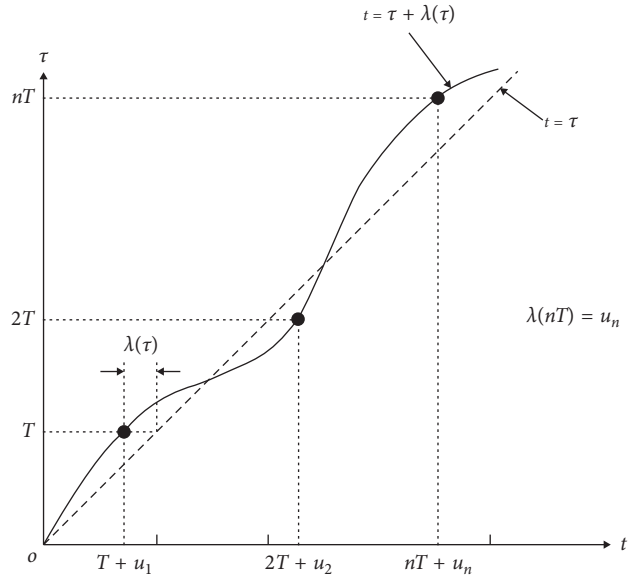

FIGURE 2: The schematic of nonlinear time transformation of BTT sampling times under speed fluctuation.

the center frequency f_0 and bandwidth B_0 in "true" blade vibration signals. Secondly, the reconstructed band-pass signal $g(\tau)$ can be represented as [13]

$$\widehat{g}(\tau) = \mathrm{Re}\left\{\sum_{m=-\infty}^{m=+\infty} \widetilde{d}(nT + u_n)\sin c\left(f_{\mathrm{BTT}}\tau - m\right) \cdot \exp\left[j2\pi f_0\left(\tau - \frac{m}{f_{\mathrm{BTT}}}\right)\right]\right\}, \tag{14}$$

where $\widetilde{d}(nT + u_n)$ is the analytic version of $d(nT + u_n)$, $\sin c$ is the cardinal sine function, f_{BTT} is the BTT sampling frequency which is calculated as $f_{\mathrm{BTT}} = I/T$, and $\mathrm{Re}\{\cdot\}$ denotes the real part.

Obviously, it can be seen from equation (14) that the band-pass signal $g(\tau)$ can be reconstructed without error from the subsampled signal $d(nT + u_n)$ under rotating speed fluctuation only if $f_{\mathrm{BTT}} > 4.26 \times B_0$ [13], where B_0 is determined by practical requirements. In order to accelerate the convergence of the summation in equation (14), polynomial splines with compact-support and excellent approximation capabilities can be used to replace the $\sin c$ function. Thus, a reconstruction kernel function $K_B[n]$ based on sixth-order B-splines is also used in this paper [13]. Finally, we can build the reconstruction formula of $g(\tau)$ as follows:

$$\widehat{g}(\tau) = \mathrm{Re}\left\{\sum_{m=-\infty}^{m=+\infty} \widetilde{d}(nT + u_n)K_B\left(f_{\mathrm{BTT}}\tau - m\right) \cdot \exp\left[j2\pi f_0\left(\tau - \frac{m}{f_{\mathrm{BTT}}}\right)\right]\right\}. \tag{15}$$

Furthermore, as shown in Figure 1, it is reasonable to assume that absolute value of sampling time variations u_n is no larger than $T/2$. Otherwise, the sampling time may be considered as the previous or the next sampling time. In this case, equation (11) is strictly monotonic, so its inverse function should exist which is defined as $\tau = \eta(t)$. Then, based on equation (15), we can obtain the BTT vibration signal reconstruction formula under uniform BTT sensor configuration and rotating speed fluctuation as follows:

$$\widehat{d}(t) = \widehat{g}(\eta(t)) = \mathrm{Re}\left\{\sum_{m=-\infty}^{m=+\infty} \widetilde{d}(nT + u_n)K_B\left[f_{\mathrm{BTT}}\eta(t) - m\right] \cdot \exp\left[j2\pi f_0\left(\eta(t) - \frac{m}{f_{\mathrm{BTT}}}\right)\right]\right\}. \tag{16}$$

Next, the remaining problem is how to calculate the inverse function $\eta(t)$. In practice, it is much difficult to get its analytical formula. But, we can obtain nT and $nT + u_n$, so $\eta(t)$ can be achieved by interpolation methods.

4.2. Nonuniform BTT Sensor Configuration. Under uniform sampling, synchronous vibrations of multiple orders of the probe number are often difficult to be detected. In order to solve this issue, nonuniformly mounted BTT probes have to be used, instead of uniformly mounted ones. Thus, we assume that the I BTT sensors are mounted nonuniformly. In this case, if the rotation speed f_{r} is constant, the nonuniform BTT sampling function can be formulated as follows:

$$\overline{d}(t) = d(t)\sum_{i=0}^{I-1}\sum_{n=0}^{N-1}\delta\left(t - \frac{n}{f_{\mathrm{r}}} - \frac{\alpha_i}{2\pi f_{\mathrm{r}}}\right), \tag{17}$$

where $d(t)$ is the true vibration signal and $\delta(\cdot)$ is the Dirac delta function.

Interestingly, it can be seen from equation (17) that nonuniformly sampled vibration signals is equivalent to the sum of I uniformly sampled signal streams. Furthermore, the reconstruction process of $d(t)$ is represented in Figure 3, which is formulated as follows [14]:

$$d_{\mathrm{re}}(t) = \sum_{i=0}^{I-1}\sum_{n=0}^{N-1} d\left(\frac{n}{f_{\mathrm{r}}} + \frac{\alpha_i}{2\pi f_{\mathrm{r}}}\right)h_i\left(t - \frac{n}{f_{\mathrm{r}}} - \frac{\alpha_i}{2\pi f_{\mathrm{r}}}\right), \tag{18}$$

where $h_i(t)$ is the i^{th} interpolating function corresponding to the i^{th} BTT sensor.

Next, the remaining problem is how to calculate the interpolating function h_i. In practice, it is much difficult to directly obtain analytical solution of h_i in time domain. To overcome it, we can perform Fourier transform on both sides of equation (18) and will have

$$D_{\mathrm{re}}(f) = \sum_{i=0}^{I-1} f_{\mathrm{r}}H_i(f)\sum_{n=-\infty}^{\infty} D(f - nf_r)e^{-jn\alpha_i}, \tag{19}$$

where $D_{\mathrm{re}}(f)$, $D(f)$, and $H_i(f)$ are the spectrums of $d_{\mathrm{re}}(t)$, $d(t)$, and $h_i(t)$, respectively.

Hu et al. proposed the method of solving $H_i(f)$ [14]. Then, we can obtain the reconstructed spectrum $D_{\mathrm{re}}(f)$ by substituting $H_i(f)$ into equation (19), leading to the solution of $d_{\mathrm{re}}(t)$. In this paper, two BTT sensors are used as an

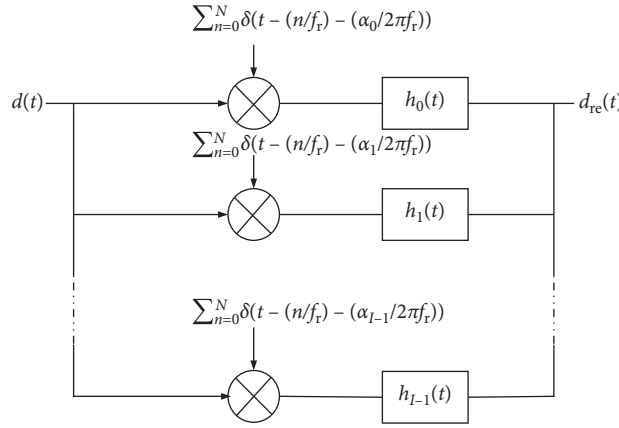

Figure 3: The schematic of periodically nonuniformly sampled signal reconstruction [14].

example. Without loss of generality, α_0 is assumed to be zero. Then, the corresponding second-order reconstruction formula is as follows [14]:

$$d_{re}(t)=\sum_{n=-\infty}^{\infty} d\left(\frac{n}{B_0}\right)h\left(t-\frac{n}{B_0}\right)+d\left(\frac{n}{B_0}+\frac{\alpha_1}{2\pi B_0}\right)h\left(-t+\frac{n}{B_0}+\frac{\alpha_1}{2\pi B_0}\right), \tag{20}$$

where

$$\begin{aligned} h(t)=&\frac{\cos\left(2\pi\left(mB_0-f_L\right)t-m\alpha_1/2\right)-\cos\left(2\pi f_L t-m\alpha_1/2\right)}{2\pi B_0 t\sin\left(m\alpha_1/2\right)}\\ &+\frac{\cos\left(2\pi\left(B_0+f_L\right)t-(m+1)\alpha_1/2\right)-\cos\left(2\pi\left(mB_0-f_L\right)t-(m+1)m\alpha_1/2\right)}{2\pi B_0 t\sin\left((m+1)m\alpha_1/2\right)}, \end{aligned} \tag{21}$$

where f_L is the lower boundary of the frequency band and $m=2f_L/B_0$. The ceiling operator X denotes the smallest integer no less than X. However, it must be noted that two important constraints should be satisfied, i.e., $\sin(m\alpha_1/2)\neq 0$ and $\sin(((m+1)\alpha_1)/2)\neq 0$. Therefore, angular positions of two BTT sensors should be selected carefully to avoid incorrect vibration reconstructions in engineering applications.

When considering rotating speed fluctuation, sampling times of the ith BTT sensor can be represented as

$$t_i=\frac{n}{\overline{f}_r}+\frac{\alpha_i}{2\pi\overline{f}_r}+u_{i,n},\quad n=0,\ldots,N-1. \tag{22}$$

Based on equation (11), nonlinear time transformation of t_i can be obtained as follows:

$$t_i=\gamma_i(\tau_i)=\tau_i+\lambda_i(\tau_i), \tag{23}$$

where $\lambda_i(n/\overline{f}_r)=u_{i,n}$. Similarly, we assumed the inverse function of $\lambda_i(\tau)$ to be $\eta_i(t)$, i.e., $\tau=\eta_i(t)$.

For each BTT sensor, it can be looked as being mounted uniformly, so we can obtain the BTT vibration signal reconstruction formula in the τ domain as follows:

$$\widehat{d}_{re}(\tau)=\sum_{i=0}^{I-1}\sum_{n=0}^{N-1} d\left(\frac{n}{\overline{f}_r}+\frac{\alpha_i}{2\pi\overline{f}_r}+u_{i,n}\right)h_i\left(\tau-\frac{n}{\overline{f}_r}-\frac{\alpha_i}{2\pi\overline{f}_r}\right). \tag{24}$$

By substituting $\tau=\eta_i(t)$ into equation (24), we can obtain the BTT vibration signal reconstruction formula under nonuniform BTT sensor configuration and rotating speed fluctuation as follows:

$$\begin{aligned} d_{re}(t)=\widehat{d}_{re}(\eta_i(t))=&\sum_{i=0}^{I-1}\sum_{n=0}^{N-1} d\left(\frac{n}{\overline{f}_r}+\frac{\alpha_i}{2\pi\overline{f}_r}+u_{i,n}\right)\\ &\cdot h_i\left(\eta_i(t)-\frac{n}{\overline{f}_r}-\frac{\alpha_i}{2\pi\overline{f}_r}\right). \end{aligned} \tag{25}$$

In particular, when $I=2$, we will have the following reconstruction formula:

$$\begin{aligned} d_{re}(t)=\sum_{n=-\infty}^{\infty}\Bigg[&d\left(\frac{n}{\overline{f}_r}+u_{1,n}\right)h\left(\eta_1(t)-\frac{n}{\overline{f}_r}\right)\\ &+d\left(\frac{n}{\overline{f}_r}+\frac{\alpha_1}{2\pi\overline{f}_r}+u_{2,n}\right)h\left(-\eta_2(t)+\frac{n}{\overline{f}_r}+\frac{\alpha_1}{2\pi\overline{f}_r}\right)\Bigg], \end{aligned} \tag{26}$$

where $d((n/\overline{f}_r) + u_{1,n})$ and $d((n/\overline{f}_r) + (\alpha_1/2\pi\overline{f}_r) + u_{2,n})$ are sampled vibration displacements by the first and second BTT sensors under rotating speed fluctuation.

5. Numerical Simulations and Validations

In order to validate the above two vibration signal reconstruction algorithms, BTT sampled signals under rotating speed fluctuation and no fluctuation are simulated, respectively. Then, both the proposed algorithm and classical methods in [10, 13] are used to reconstruct them. Finally, the original signals are compared with the reconstructed signals and the corresponding evaluation metrics is calculated.

5.1. Under Uniform BTT Sensor Configuration and Rotating Speed Fluctuation. Without loss of generality, it is assumed that three fault frequencies are caused by blade damages, i.e., $f_1 = 800$ Hz, $f_2 = 760$ Hz, and $f_3 = 850$ Hz. Then, the characteristic vibration signal can be represented as

$$d(t) = \sin(2\pi f_1 t) + 0.5\sin(2\pi f_2 t + 39) + 0.3\sin(2\pi f_3 t + 95). \quad (27)$$

Under rotating speed fluctuation, the average rotating speed is equal to 5000 RPM and then $\overline{f}_r = 83.33$ Hz and $T = 3/250$ s. Three BTT sensors are mounted equally, and the BTT sampling frequency can be calculated as $f_{BTT} = 250$ Hz. The total sampling time is equal to 5 seconds. The rotating speed fluctuation is assumed to be random normal distribution. Here, two kinds of fluctuations with URS = 3.16% and URS = 6.33% are studied, respectively. Then, the rotating speed and the variation of sampling time are shown in Figure 4. Based on them, the sampling times $nT + u_n$ can be obtained and the sampled vibration displacements $d(nT + u_n)$ under rotating speed fluctuation can also be calculated, which are shown in Figure 5.

Based on Figures 4 and 5, it can be seen that the sampling times and sampled vibration displacements are a little different under two rotating speed fluctuations. Next, under rotating speed fluctuation, classical and the proposed NTT-based methods are used to recover characteristic vibration frequencies, respectively, which are compared with those under constant rotating speed. For the reconstruction, the targeted central frequency is chosen as $f_0 = 800$ Hz. The bandwidth is chosen as $B_0 = 55$ Hz so that $f_{BTT} > 4.26 \times B_0$. Furthermore, we need to calculate the inverse function $\eta(t)$ by the interpolation method. It can be testified that $|\lambda| < T/2$, so here we obtain $\eta(t)$ by the one-dimensional linear interpolation method. In the end, reconstructed signals under uniform sampling using classical method under fluctuation and using the proposed NTT-based method under fluctuation are calculated, respectively, and compared in Figure 6. Obviously, it is difficult to distinguish them in time domain. Furthermore, their power spectrums are calculated as in Figure 7. It can be seen that when URS = 3.16%, the reconstructed vibration frequencies are calculated as 760.2 Hz, 800.2 Hz, and 850.2 Hz using the classical reconstruction algorithm. While using the proposed NTT-based reconstruction algorithm, the reconstructed vibration frequencies are the same as the original values. When URS = 6.33%, however, it is difficult to determine reconstructed vibration frequencies by using the classical reconstruction algorithm. While the proposed NTT-based reconstruction algorithm can still be used to accurately reconstruct the original characteristic frequencies.

Furthermore, the metric of normalized spectral kurtosis is used to measure the reconstruction performance. In the case of URS = 3.16%, we will have $S_k = 0.4263$ by using the classical method under fluctuation and $S_k = 0.9967$ by using the proposed method under fluctuation, respectively. While in the case of URS = 6.33%, we will have $S_k = 0.1048$ by using classical method under fluctuation and $S_k = 0.9836$ by using the proposed method under fluctuation, respectively. Thus, the results testify that the NTT-based reconstruction method can reduce effectively the influence of rotating speed fluctuation and decrease the reconstruction error.

In order to evaluate the effect of URS on the performance of the NTT-based reconstruction method, the above reconstruction process is done under different URS. Here, the URS changes between 1% and 35%. Then, the corresponding normalized spectral kurtosis of reconstructed signals is calculated and the results are shown in Figure 8. It can be seen that (1) when URS > 5%, the normalized spectral kurtosis obtained by using classical method will decrease sharply and be less than 0.2. While the normalized spectral kurtosis obtained by using the NTT-based method will be large than 0.8 only if URS ≤ 25%. (2) When URS > 30%, the normalized spectral kurtosis obtained by using the NTT-based method will also decrease sharply. At this time, however, the rotating speed will be seen as to be variable, instead of fluctuation. Thus, we can conclude that the NTT-based reconstruction method is much fit for BTT vibration reconstruction under uniform sensor configuration and rotating speed fluctuation.

5.2. Under Nonuniform BTT Sensor Configuration and Rotating Speed Fluctuation. As mentioned before, nonuniform BTT sensor configuration is always utilized to monitor synchronous vibrations. In this section, simulations are done to validate the proposed reconstruction method in Section 4.2. Here, two BTT sensors are mounted nonuniformly, and the angle between them is equal to 30 degree.

It is assumed that synchronous vibration frequency is equal to $f_1 = 800$ Hz and asynchronous vibration frequencies are equal to $f_2 = 780$ Hz and $f_3 = 810$ Hz. Then, the characteristic vibration signal can be similarly generated based on equation (27).

In particular, a revolution reference sensor is mounted to collect rotating speed signals in order to obtain practical fluctuation. In order to simulate practical rotating speed fluctuation, here an experimental rotating speed is used and shown in Figure 9, which was measured by a rotating speed sensor. The average speed is equal to 5019.8 rpm. Furthermore, we will have $\overline{f}_r = 83.66$ Hz and URS = 0.82%.

Next, the average speed is used to calculate the BTT sampling times under no fluctuation. Based on this, the variation of BTT sampling time is shown in Figure 10. Then,

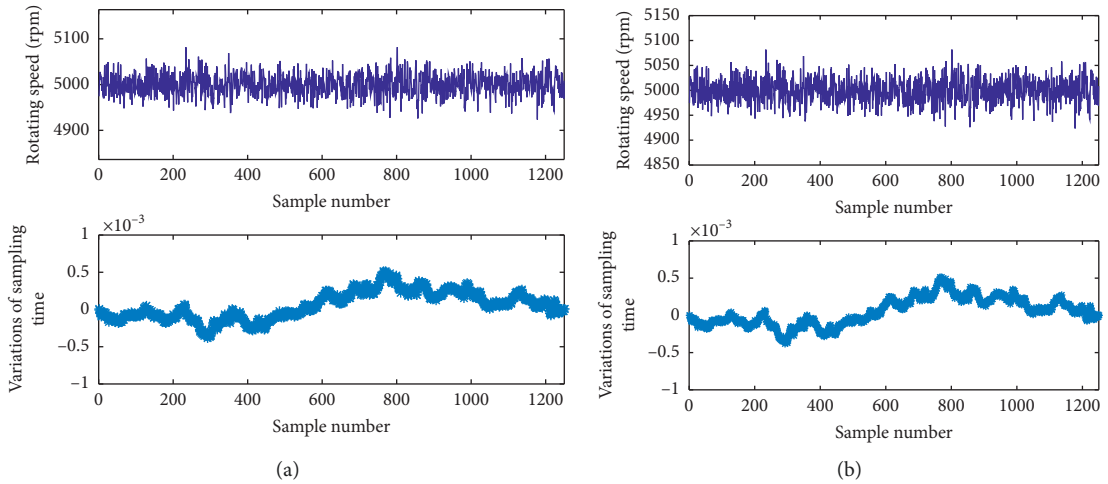

Figure 4: Stochastic speed fluctuation and variations of BTT sampling time: (a) URS = 3.16%; (b) URS = 6.33%.

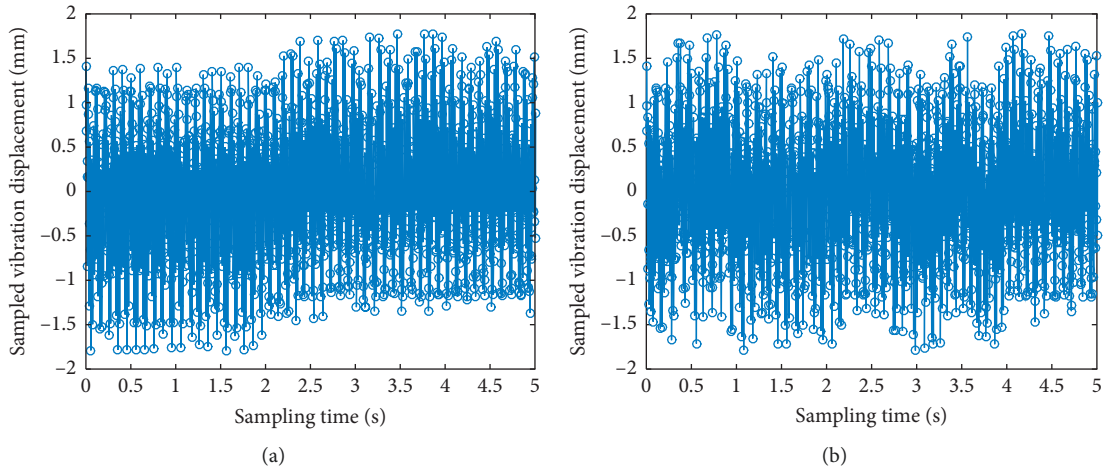

Figure 5: Sampled vibration displacements under rotating speed fluctuation: (a) URS = 3.16%; (b) URS = 6.33%.

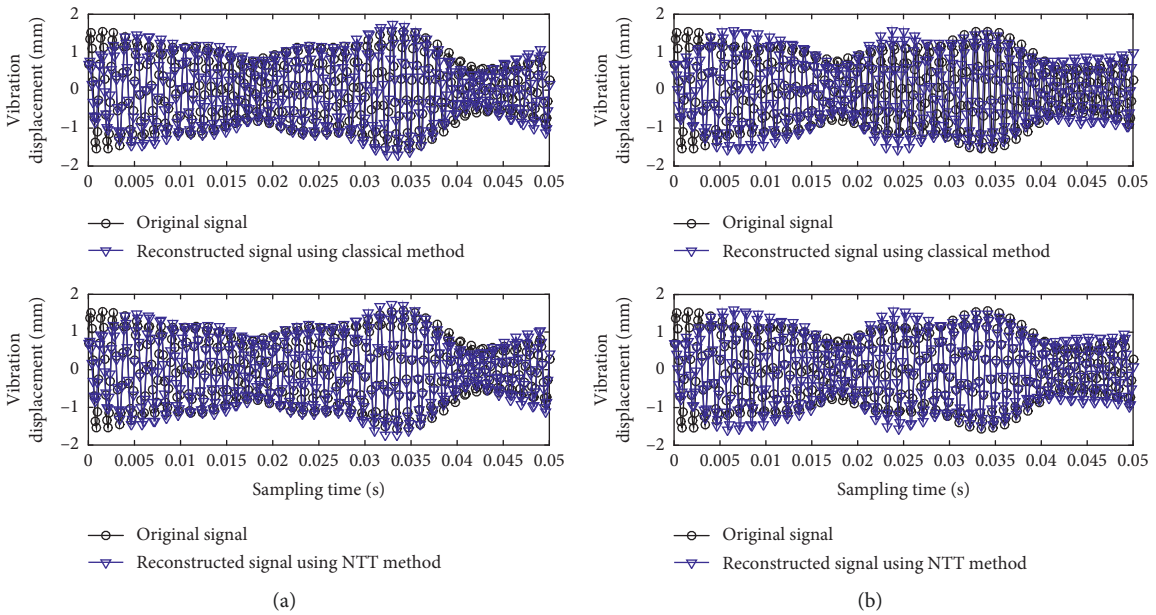

Figure 6: Continued.

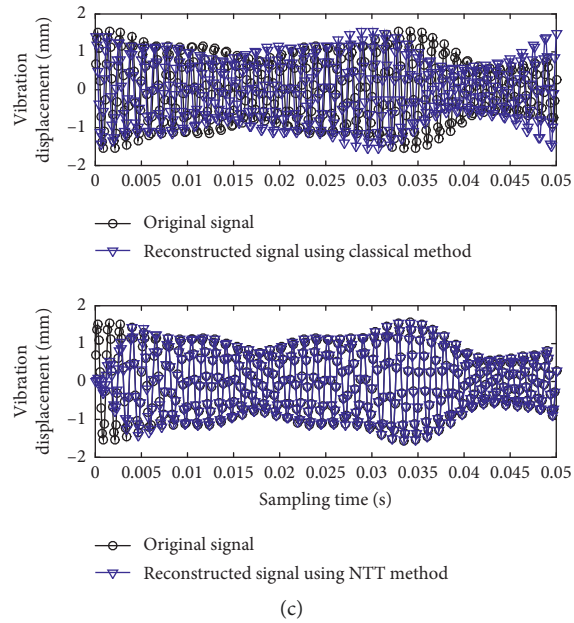

(c)

Figure 6: Comparisons of original and reconstructed vibration displacements: (a) URS = 3.16%; (b) URS = 6.33%; (c) URS = 0%.

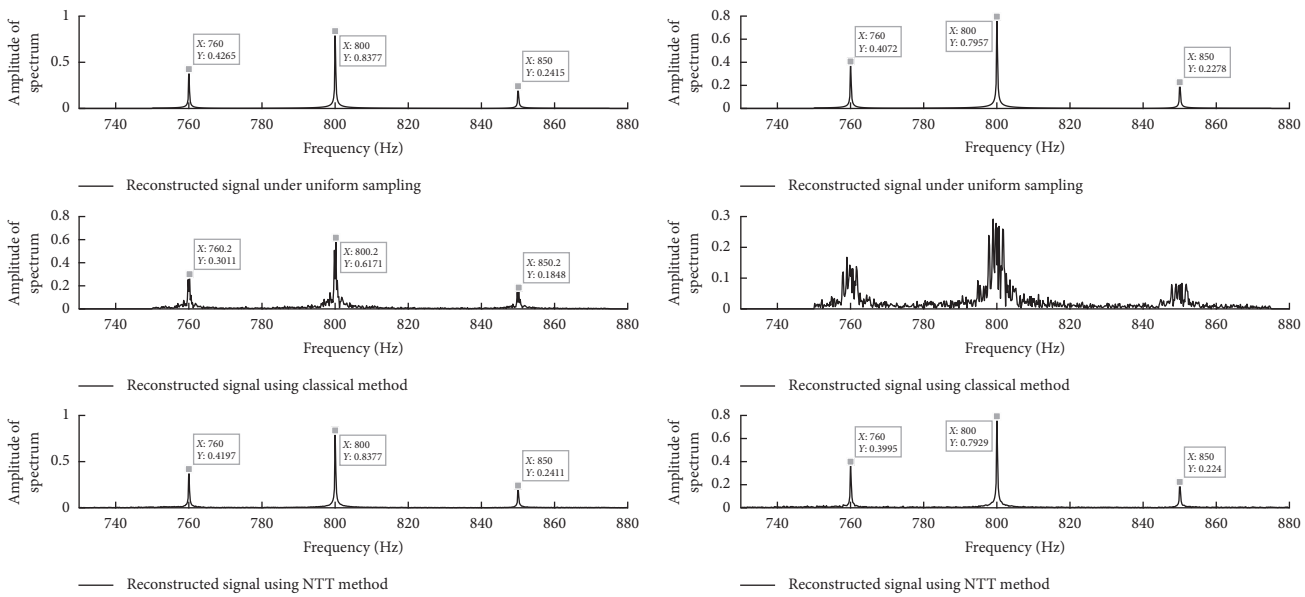

(a) (b)

Figure 7: Comparisons of reconstructed vibration spectrums using different methods: (a) URS = 3.16%; (b) URS = 6.33%.

nonlinear transformation transformations are done, and the inversion functions $\eta_1(t)$ and $\eta_2(t)$ in equation (26) are calculated and shown in Figure 11, respectively. Here, the URS is too small, so the two curves seem to be a straight line. Furthermore, $h(t)$ in equation (26) can be calculated and is shown in Figure 12.

In the end, the reconstruction formula in equation (26) is used to reconstruct the characteristic vibration signal. In order to evaluate the performance, the results of the NTT-based method are compared with those of classical method, as shown in Figure 13. For clarity of display, only the waveform among [0, 0.1] ms along the time axis is drawn. The reconstruction results under no fluctuation are shown in Figure 13(a). The reconstruction results under fluctuation by using classical and NTT-based method are shown in Figures 13(b) and 13(c), respectively. The original signals are obtained by instituting sampling times in Figure 10 into equation (27). It can be seen that the reconstructed spectrum obtained by the NTT-based method under fluctuation is almost the same as that under no fluctuation, so we can easily find one synchronous vibration frequency (800 Hz) and the two synchronous vibration frequencies (780 Hz and 810 Hz). While for the reconstructed spectrum obtained by classical method under fluctuation, there are much spectral leakages

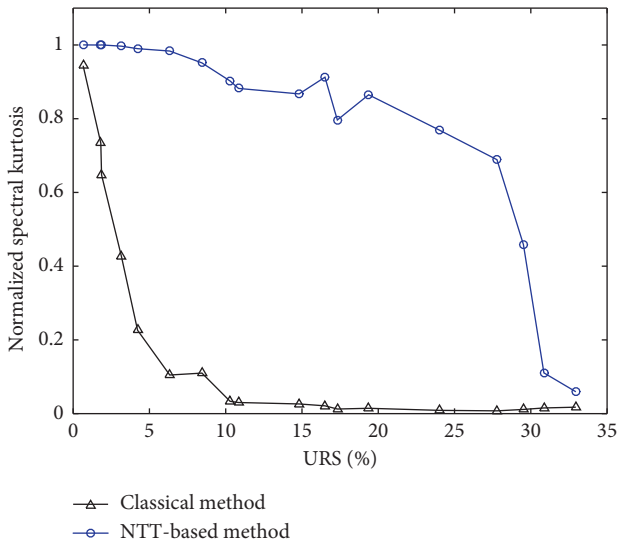

Figure 8: Normalized spectral kurtosis of uniformly reconstructed signals under different URS.

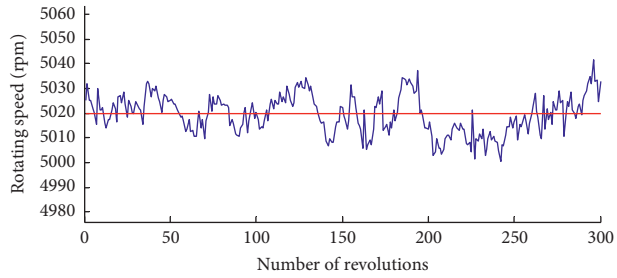

Figure 9: Experimental rotating speed.

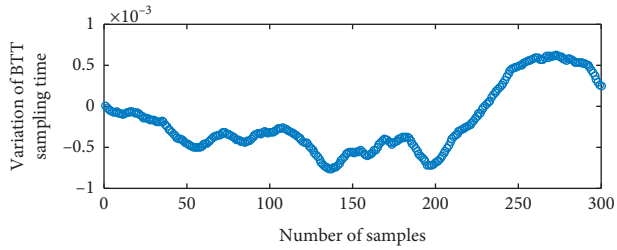

Figure 10: The variation of BTT sampling time using experimental rotating speed.

despite of small URS. Thus, we can believe that the classical method cannot be used for BTT vibration reconstruction if URS is larger.

Similarly, in order to evaluate the effect of URS on the performance of the NTT-based reconstruction method under fluctuation, the above reconstruction method is carried out under different URS. Then, the corresponding normalized spectral kurtosis of reconstructed signals is calculated and shown in Figure 14. It can be seen that (1) when URS increases to be more than 0.8%, the normalized spectral kurtosis obtained by using classical method will decrease sharply and be less than 0.2. While the normalized spectral kurtosis obtained by using the NTT-based method will be large than 0.8 until URS > 8.3%. Thus, it validates that

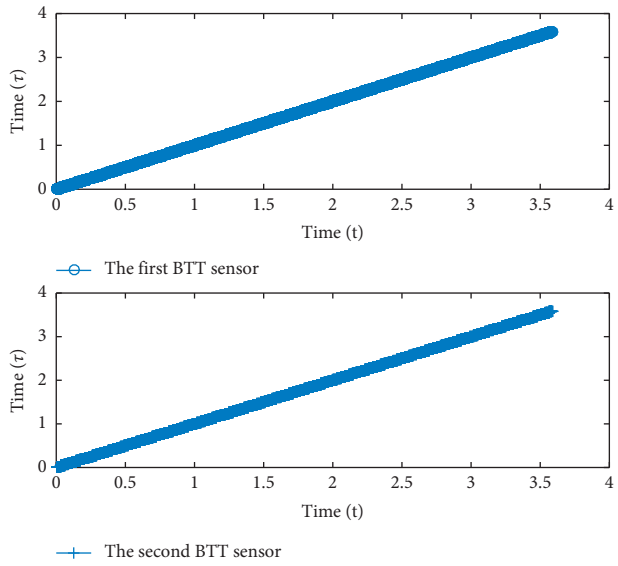

Figure 11: The two inverse functions in equation (26).

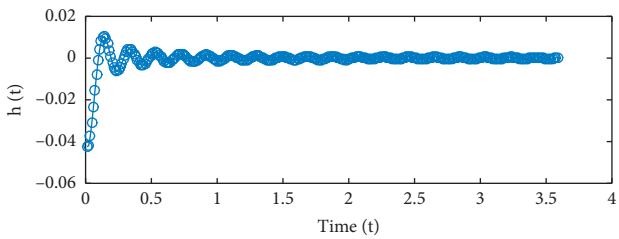

Figure 12: The interpolation function in equation (26).

the proposed method is more insensitive to speed fluctuation than classical method. (2) By comparing Figure 14 with Figure 8, we can see that speed fluctuation has more bad effects on both reconstruction methods under nonuniform sensor configuration than under uniform sensor configuration. (3) Similarly, when URS > 10%, the normalized spectral kurtosis obtained by using the NTT-based method will also decrease sharply.

5.3. Improper Angles between Two BTT Sensors. As mentioned before, there are some improper angles between BTT sensors for nonuniform BTT signal reconstructed by using the NTT-based method. Furthermore, these improper angles can be calculated to avoid large reconstruction errors once the rotating speed and the targeted central frequency are given. Here, the average rotating speed is equal to 5020 rpm, and the targeted central frequency is equal to 800 Hz. The reconstruction bandwidth is $B = 5020/60 = 83.67$ Hz. Based on them, we will have $f_L = f_0 - B/2 = 758.17$ Hz and $m = \text{ceil}(2f_L/B) = 19$. Then, angles between two BTT sensors (α_1) should satisfy $\alpha_1 \neq 2k\pi/19$ and $\alpha_1 \neq k\pi/10$, where k is an integer. Furthermore, the set of improper angles can be listed as {18°, 18.9°, 36°, 37.9°, 54°, 56.8°, 72°, 75.8°, 90°, 94.7°, 108°, 113.7°, 126°, 132.6°, 144°, 151.6°, 162°, 170.5°}. In order to validate this conclusion, next numerical simulations are done as follows.

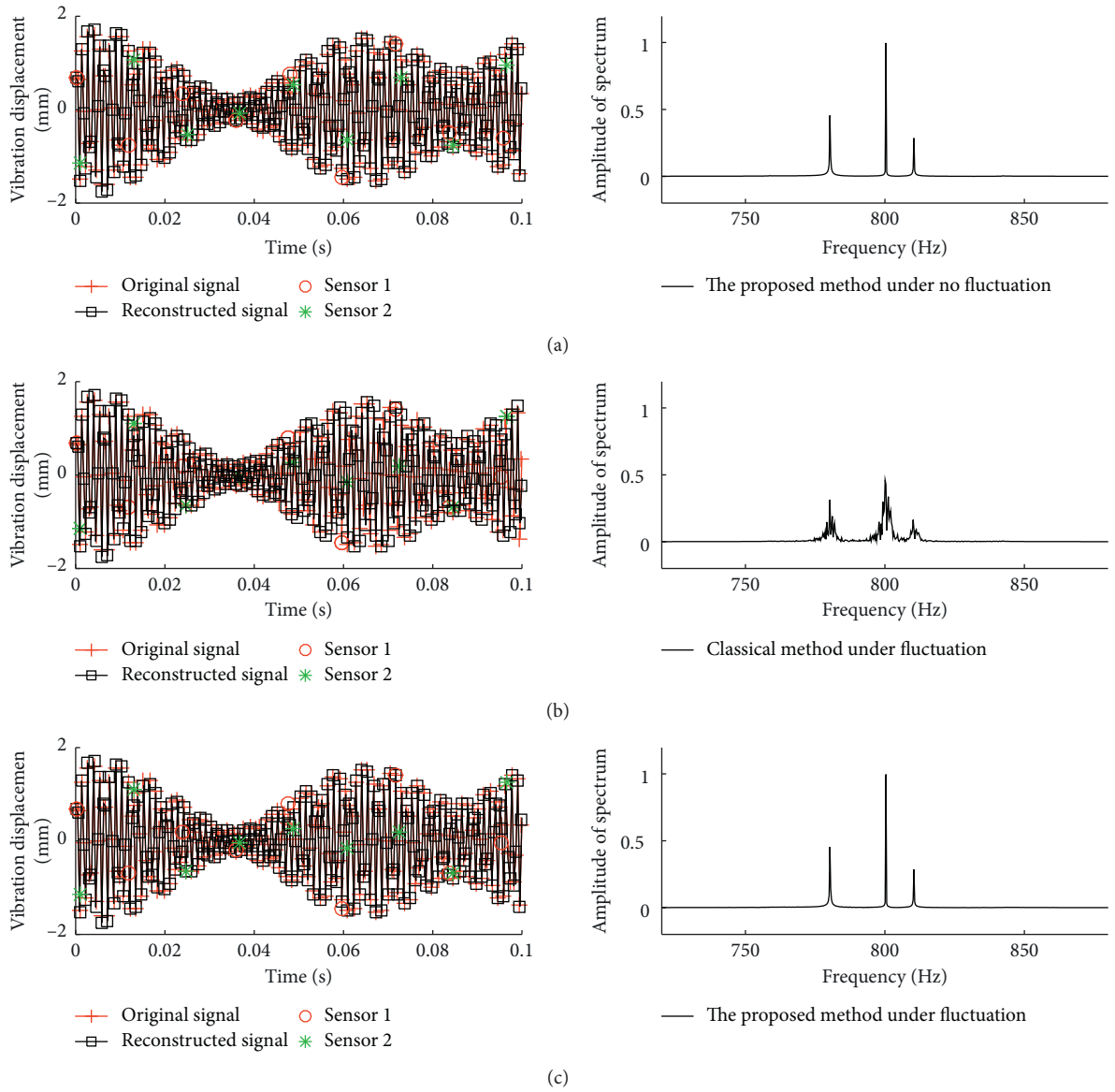

Figure 13: Comparisons of reconstructed vibrations by two methods.

Here, URS = 0.82%. Then normalized spectral kurtosis of nonuniformly reconstructed signals under different α_1 are calculated by using the NTT-based method, respectively. The results are shown in Figure 15. We can see that (i) in most cases, α_1 has few effects on the performance of the proposed reconstruction method, except for some improper angles which are equal to the above theoretic values. (ii) When improper α_1 is used, the performances of the NTT-based method will decrease greatly. Thus, for nonuniform BTT signal reconstruction under rotating speed fluctuation, more attentions should be paid on selecting right angles between two BTT sensors.

6. Conclusions

BTT-based vibration signals are typically undersampled, so it is much necessary to reconstruct characteristic vibrations. Existing reconstruction methods are mainly based on the assumption of constant rotation speeds. But, rotating speed fluctuation is inevitable in engineering applications due to unstable airflow, load instability, and other factors. In this case, blade vibrations cannot be reconstructed accurately by using existing algorithms, so that frequency aliasing will happen. Thus, the aim of this paper is to explore a new BTT vibration reconstruction method under rotating speed fluctuation. Main contributions of this paper can be summarized as follows: (1) effects of rotating speed fluctuation on BTT vibration reconstruction are analyzed, and nonlinear time transformation of BTT sampling times under rotating speed fluctuation is presented. (2) Two NTT-based reconstruction algorithms are derived for uniform and nonuniform BTT sensor configurations, respectively. (3) Numerical simulations are done to verify the proposed methods. The results testify that the proposed NTT-based reconstruction method can reduce effectively the influence of rotating speed fluctuation and decrease the reconstruction

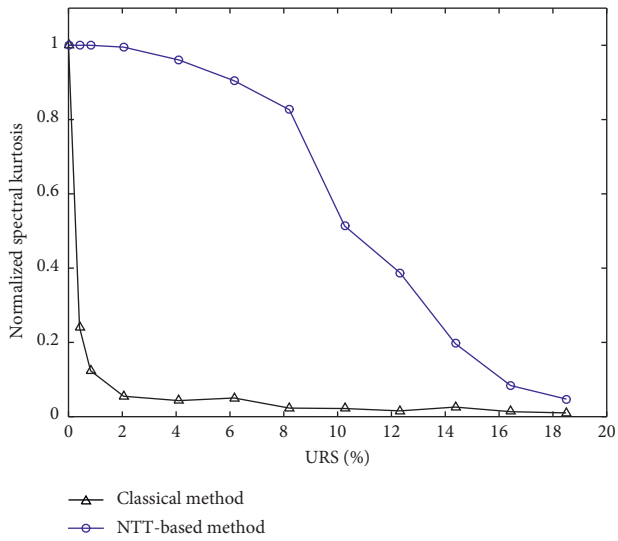

Figure 14: Normalized spectral kurtosis of nonuniformly reconstructed signals under different URS.

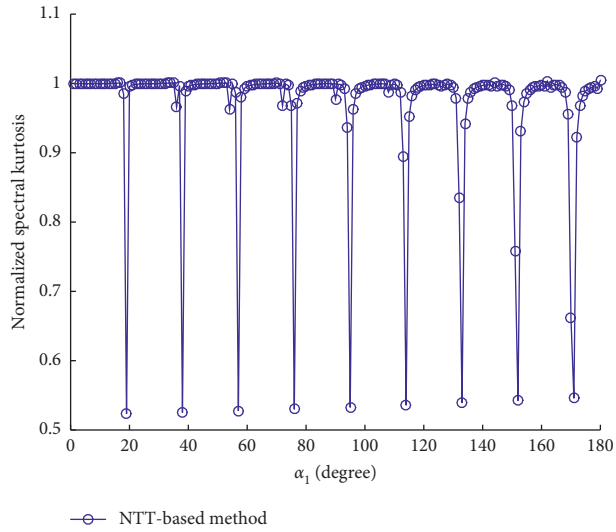

Figure 15: Normalized spectral kurtosis of nonuniformly reconstructed signals under different α_1 values.

error. In addition, rotating speed fluctuation has more bad effects on reconstruction methods under nonuniform sensor configuration than under uniform sensor configuration. For nonuniform BTT signal reconstruction under rotating speed fluctuation, more attentions should be paid on selecting proper angles between BTT sensors. The proposed method will benefit for detecting early blade damages by reducing frequency aliasing. In addition, it must be noted that if rotating speeds change too much, the performance of the proposed algorithms will also decrease greatly. Thus, another future work is to study BTT-based vibration signal reconstruction methods under variable rotating speeds [16].

Data Availability

The data used to support the findings of this study are available from the corresponding authors upon request.

Conflicts of Interest

The authors declare that there are no conflicts of interests regarding the publication of this paper.

Acknowledgments

This work was supported by the National Basic Research Program of China (Grant No. 2015 CB057400).

References

[1] R. Fleeting and R. Coats, "Blade failures in the HP turbines of RMS Queen Elizabeth and their rectification," *Transactions Institute of Marine Engineers*, vol. 82, pp. 49–74, 1970.

[2] H. L. Xu, Z. S. Chen, Y. P. Xiong, Y. M. Yang, and L. M. Tao, "Nonlinear dynamic behaviors of rotated blades with small breathing cracks based on vibration power flow analysis," *Shock and Vibration*, vol. 2016, Article ID 4197203, 11 pages, 2016.

[3] Z. Chen, J. He, J. Liu, and Y. Xiong, "Switching delay in self-powered nonlinear piezoelectric vibration energy harvesting circuit: mechanisms, effects, and solutions," *IEEE Transactions on Power Electronics*, vol. 34, no. 3, pp. 2427–2440, 2019.

[4] W. Wang, Q. Li, J. Gao, J. Yao, and P. Allaire, "An identification method for damping ratio in rotor systems," *Mechanical Systems and Signal Processing*, vol. 68-69, no. 2, pp. 536–554, 2016.

[5] A. Ghoshal, M. J. Sundaresan, M. J. Schulz, and P. Frank Pai, "Structural health monitoring techniques for wind turbine blades," *Journal of Wind Engineering and Industrial Aerodynamics*, vol. 85, no. 3, pp. 309–324, 2000.

[6] C. Lawson and P. Ivey, "Tubomachinery blade vibration amplitude measurement through tip timing with capacitance tip clearance probes," *Sensors and Actuators A: Physical*, vol. 118, no. 1, pp. 14–24, 2005.

[7] J. Lin, Z. Hu, Z.-S. Chen, Y.-M. Yang, and H.-L. Xu, "Sparse reconstruction of blade tip-timing signals for multi-mode blade vibration monitoring," *Mechanical Systems and Signal Processing*, vol. 81, no. 12, pp. 250–258, 2016.

[8] J. Gallego-Garrido, G. Dimitriadis, and J. R. Wright, "A class of methods for the analysis of blade tip timing data from bladed assemblies undergoing simultaneous resonances-Part I: theoretical development," *International Journal of Rotating Machinery*, vol. 2007, Article ID 27247, 11 pages, 2007.

[9] I. B. Carrington, J. R. Wright, J. E. Cooper, and G. Dimitriadis, "A comparison of blade tip timing data analysis methods," *Proceedings of the Institution of Mechanical Engineers, Part G: Journal of Aerospace Engineering*, vol. 215, no. 5, pp. 301–312, 2001.

[10] S. Bendali, L. Joseph, B. Marc, V. Philippe, and B. Charles, "Modal parameter identification of mistuned bladed disks using tip timing data," *Journal of Sound and Vibration*, vol. 314, no. 3–5, pp. 885–906, 2008.

[11] Z. S. Chen, Y. M. Yang, B. Guo, and Z. Hu, "Blade damage prognosis based on kernel principal component analysis and grey model using subsampled tip-timing signals," *Proceedings of the Institution of Mechanical Engineers Part C-Journal of Mechanical Engineering*, vol. 228, no. 17, pp. 3178–3185, 2014.

[12] A. Bouchain, J. Picheral, E. Lahalle, A. Vercoutter, and A. Talon, "Sparse method for tip-timing signals analysis with non stationary engine rotation frequency," in *Proceedings of*

the 26th European Signal Processing Conference (EUSIPCO 2018), Rome, Italy, September 2018.

[13] Z. S. Chen, Y. M. Yang, Y. Xie, and Z. Hu, "Non-contact crack detection of high-speed blades based on principal component analysis and Euclidian angles using optical-fiber sensors," *Sensors and Actuators A: Physical*, vol. 201, no. 10, pp. 66–72, 2013.

[14] Z. Hu, J. Lin, Z.-S. Chen, Y.-M. Yang, and X.-J. Li, "A non-uniformly under-sampled blade tip-timing signal reconstruction method for blade vibration monitoring," *Sensors*, vol. 15, no. 2, pp. 2419–2437, 2015.

[15] A. Papoulis, "Error analysis in sampling theory," *Proceedings of the IEEE*, vol. 54, no. 7, pp. 947–955, 1966.

[16] Z. S. Chen, J. H. Liu, C. Zhan, J. He, and W. M. Wang, "Reconstructed order analysis-based vibration monitoring under variable rotation speed by using multiple blade tip-timing sensors," *Sensors*, vol. 18, no. 10, p. 3235, 2018.